Translating intracellular calcium signaling into models

Rüdiger Thul[*]
School of Mathematical Sciences, University of Nottingham, Nottingham, NG7 2RD, United Kingdom

Abstract

The rich experimental data on intracellular calcium has put theoreticians in an ideal position to derive models of intracellular calcium signaling. Over the last 25 years, a large number of modeling frameworks have been suggested. Here, I will review some of the milestones of intracellular calcium modeling with a special emphasis on calcium-induced-calcium release (CICR) through inositol-1,4,5-trisphosphate and ryanodine receptors. I will highlight key features of CICR and how they are represented in models as well as the challenges that theoreticians face when translating our current understanding of calcium signals into equations. The selected examples demonstrate that a successful model provides mechanistic insights into the molecular machinery of the Ca^{2+} signaling toolbox and determines the contribution of local Ca^{2+} release to global Ca^{2+} patterns, which at the moment cannot be resolved experimentally. The protocols in this chapter provide introductory examples to modeling CICR, which may serve as a starting point for theoretically exploring the wealth of intracellular calcium signals and link it to experimental data.

Introduction

One of the most fascinating features of calcium (Ca^{2+}) as a second messenger is its versatility (Berridge et al. 2000). Almost every cell type shows Ca^{2+} signals, and even within a single cell the number of signaling pathways that involve Ca^{2+} is huge. From a modeler's perspective the broad spectrum of interactions renders Ca^{2+} an intriguing yet challenging study object. The fascination originates from the large dynamic repertoire of Ca^{2+} signals. Most Ca^{2+} responses begin with the elevation of the cytosolic Ca^{2+} concentration through either Ca^{2+} entry from the extracellular space or Ca^{2+} liberation from intracellular organelles such as the endoplasmic or sarcoplasmic reticulum (ER/SR). Although the molecular details of the ion channels that are responsible for the increase in the cytosolic Ca^{2+} concentration differ, in all cases, Ca^{2+} forms a plume of high concentration around the site of influx just after a channel opens. These microdomains form the smallest functional unit of intracellular Ca^{2+} signals (Berridge 2006) from which larger Ca^{2+} patterns are formed. For example, it is the orchestrated action of microdomains that gives rise to cellular responses such as Ca^{2+} waves and Ca^{2+} oscillations (Bootman et al. 1997). Some Ca^{2+} waves travel through the entire cell, while others only spread through parts of the

[*] ruediger.thul@nottingham.ac.uk, tel: +44 115 8467913, fax: +44 115 9513837

cytoplasm resulting in abortive waves. The existence of Ca^{2+} microdomains and Ca^{2+} waves already points to a defining characteristic of intracellular Ca^{2+} signals – they vary largely in their temporal duration and their spatial spread. On the temporal scale, intracellular Ca^{2+} signals range from events faster than microseconds (binding and unbinding of Ca^{2+} to target molecules), to cellular Ca^{2+} transients that last minutes (Ca^{2+} waves and oscillations). At the same time, intracellular Ca^{2+} operates on length scales from a few nanometers (molecular binding sites) up to hundreds of micrometers (Ca^{2+} waves). The challenge for modelers arises from the realization that a complete account of intracellular Ca^{2+} requires us to incorporate the entire spatio-temporal spread, i.e. more than eight orders of magnitude in space and over six orders of magnitude in time.

The large range of length and time scales of intracellular Ca^{2+} patterns has led to various modeling approaches. A common research practice has been to focus on one class of Ca^{2+} signals at a time. For example, detailed investigations of the inositol-1,4,5-trisphosphate (IP_3) receptor (IP_3R) have been conducted that have greatly facilitated our mechanistic understanding of localized Ca^{2+} release events such as Ca^{2+} blips and puffs (Thul and Falcke 2004a; Shuai et al. 2007; Rüdiger et al. 2007; Taufiq-Ur-Rahman et al. 2009; Thul et al. 2009b; Swaminathan et al. 2009). More recently, a number of studies have addressed the interaction between different levels of the Ca^{2+} signaling hierarchy in a three dimensional cellular environment. To cope with the increased computational demand of simulating three spatial dimensions, all approaches had to introduce approximations. For instance, the coupling between IP_3R clusters with a detailed stochastic gating scheme for the receptor was achieved at the cost of a small number of IP_3R clusters and an idealized spherical cellular geometry (Skupin and Falcke 2009; Skupin et al. 2010; Thurley and Falcke 2011). In a study of an atrial myocytes (Thul et al. 2012), the authors employed a realistic distribution of ryanodine receptor (RyR) clusters but a simplified threshold dynamics for Ca^{2+} liberation. By focusing on a small number of RyR clusters in a cardiac myocyte, Izu *et al.* could incorporate detailed stochastic dynamics for RyRs (Izu et al. 2006). A combination of a small number of IP_3R clusters and an approximation of the Ca^{2+} concentration profile around a cluster was studied in Solovey *et al.* (2008). In contrast to the spatially extended models, each Ca^{2+} ion is treated separately in a fully stochastic simulation for a point model of a hepatocyte in (Dupont et al. 2008).

In this chapter, I will illustrate modeling concepts and applications with Ca^{2+} liberation from the ER or SR through either the IP_3R or the RyR. The main motivation for this selection comes from the fact that these receptors present an integral component in the generation of Ca^{2+} waves and oscillations, and therefore are vital for mounting a physiological response to extracellular stimuli (Thul et al. 2008a; Dupont et al. 2011; Parekh 2011). It is worth noting that IP_3Rs and RyRs differ significantly from each other in their molecular structure, their gating properties and expression patterns (Foskett et al. 2007; Zalk et al. 2007). Different tissues and cell-lines express various isoforms, each tailored to specific signaling needs. Therefore conclusions drawn for the IP_3R cannot necessarily be transferred to the RyR.

The modeling studies mentioned above highlight some of the latest developments in a long evolution of Ca^{2+} models. In what follows I will describe

three modeling approaches of increasing complexity that are stepping stones towards the more sophisticated modeling frameworks that we use today.

The well stirred cell

A common and historically an often used assumption is that a cell presents a well-stirred bioreactor. In this setting, the Ca^{2+} concentration is the same at all points within each cellular compartment such as the cytosol, the ER/SR or across all mitochondria. From a mathematical point of view, this translates into describing the dynamics of the Ca^{2+} concentration in each compartment with an ordinary differential equation (ODE). For example, the rate of change of the cytosolic Ca^{2+} concentration (c) equals the sum of all Ca^{2+} fluxes into the cytoplasm (J_{in}) minus the sum of all Ca^{2+} fluxes out of the cytosol (J_{out}):

$$\frac{\mathrm{d}c}{\mathrm{d}t} = J_{in} - J_{out}. \qquad (1)$$

This simple relation has spawned a large number of cellular Ca^{2+} models, most of which differ in the details of the Ca^{2+} influx. Assuming that the main contribution to changes in the intracellular Ca^{2+} concentration results from the IP_3R, various schemes have been put forward for the receptor as outlined in e.g. (Meyer and Stryer 1988; Goldbeter et al. 1990; De Young and Keizer 1992; Li and Rinzel 1994; Sneyd and Dufour 2002; Mak et al. 2003) and see (Sneyd and Falcke 2005) for a review. The value of all of these IP_3R models is that they provide different mechanistic interpretations of the experimental data sets that they were fitted to. Some of these models assume that Ca^{2+} and IP_3 can associate in any order with their respective binding sites, while other models stipulate a strict sequential binding order or an allosteric transformation to the active state.

Another assumption of such models is that a given value of the cytosolic Ca^{2+} concentration results in exactly one fraction of active IP_3Rs, i.e. the Ca^{2+} release flux through the IP_3R is completely *deterministic*. However, this is in stark contrast to experiments in e.g. *Xenopus* oocytes that showed the spontaneous emergence of Ca^{2+} puffs (Parker and Yao 1996; Sun et al. 1998). To reflect such random initiation of Ca^{2+} liberation, modelers replaced the deterministic Ca^{2+} flux through the IP_3R with a *stochastic* function. The simplest implementation of this modeling approach is to take any of the deterministic ODE models listed above and change the description of the IP_3R Ca^{2+} flux to its stochastic counterpart by treating the IP_3R as a Markov chain (Shuai and Jung 2002).

While ODE models of intracellular Ca^{2+} dynamics – whether deterministic or stochastic – have proven popular in the past, the richness of new experimental data prompts questions about the validity of this approach. A different interpretation of an ODE representation of the intracellular Ca^{2+} dynamics is that the equation describes the average Ca^{2+} concentration in the cell. This is indeed a good approximation if the Ca^{2+} concentration varies marginally across the cell and hence every point in the cell experiences an almost identical Ca^{2+} concentration. However, the presence of spatially localized IP_3R clusters and Ca^{2+} microdomains already indicates that the Ca^{2+} concentration can change drastically from one part of the cell to another. For example, the cytosolic Ca^{2+} concentration rises to more than 150µM at an open IP_3R cluster, while the basal Ca^{2+} concentration is around 50-150nM (Thul and Falcke 2004a). This represents more than 3 orders of magnitude, and given the sharp gradients of

the Ca^{2+} concentration around an active IP_3R cluster, averaging does not capture the true concentration profiles. The issue of largely distinct Ca^{2+} concentrations also affects the mechanistic interpretation of ion channel models. Based on thermodynamic principles, the binding rate of Ca^{2+} to a designated binding site is proportional to the Ca^{2+} concentration. Averaged Ca^{2+} concentrations usually peak around 2μM. Since realistic values of the Ca^{2+} concentration may exceed the average by a factor of 100, the binding rate is 100 times faster in the latter case than in the former. This has important consequences for processes such as Ca^{2+} induced activation or Ca^{2+} induced inhibition. Only realistic values of the cellular Ca^{2+} concentration can unravel the mechanistic details of Ca^{2+} dependent molecules and in turn faithfully represent the cellular Ca^{2+} dynamics.
It is worth remembering that models are designed to answer a particular research question and to make predictions. Models should not be limited to reproducing experimental findings. Often, an ODE model for averaged Ca^{2+} concentrations provides preliminary insights into the problem at hand and guides researchers towards more sophisticated approaches. From a practical point of view, ODE models frequently serve as a starting point to explore new signaling pathways, partly because there might not be sufficient experimental data to construct a more detailed Ca^{2+} model, and partly because the mathematical analysis of ODEs is well established and computationally cheap. Moreover, powerful analytical tools exist that give deeper insights into the mathematical details of such models. Therefore ODE models for the averaged Ca^{2+} concentration may prove useful, despite being a poor reflection of the underlying physiology.

From one compartment to the next

It became apparent early on that for models of cardiac action potentials and for local control models of excitation-contraction coupling that averaged Ca^{2+} concentrations across the cell presented a poor description of the cellular environment (DiFrancesco and Noble 1985; Stern 1992). The latter serves as a prime example of how details of the spatial arrangement of Ca^{2+} conducting ion channels lead to predictive modeling. To trigger contraction, Ca^{2+} enters the cell through L-type voltage dependent Ca^{2+} channels (VDCCs) upon depolarization of the plasma membrane. In turn, RyRs open through Ca^{2+}-induced Ca^{2+} release (CICR) (Bers 2002). A key feature of VDCCs and RyRs is that they often co-localize within a distance of approximately 15nm, hence providing RyRs with a privileged access to the Ca^{2+} influx through VDCCs. It is this localized Ca^{2+} entry that controls CICR, not a whole cell averaged L-type Ca^{2+} current. Indeed, excitation-contraction coupling can only be explained through a spatially non-uniform distribution of VDCCs-RyRs clusters (Soeller and Cannell 2004; Cannell and Kong 2012). Such spatial heterogeneity is also at the heart of the model by DiFrancesco and Noble (DiFrancesco and Noble 1985). To reproduce experimental time courses of the intracellular Ca^{2+} concentration, the authors had to assume two compartments within the SR: one pool that resequesters Ca^{2+} from the cytosol and one pool that releases Ca^{2+} into the cytosol. This highlights what is known as compartmentalized modeling. In Stern's model the two conceptual compartments are the dyadic cleft and the bulk cytosol, while DiFrancesco and Noble distinguish between the junctional and non-junctional SR

as well as the bulk cytosol. Note that compartmentalized models differ from whole cell models introduced in the previous section because they allow the division of morphologically continuous cellular compartments into functional subspaces (e.g. junctional and non-junctional SR). In turn, this leads to spatially varying Ca^{2+} concentrations as opposed to spatially homogenous Ca^{2+} concentrations in the well-stirred cell. From a mathematical point of view, compartmentalized models take on the form of coupled ODEs between the different compartments. For example, the model in (DiFrancesco and Noble 1985) can be written as

$$\frac{dc}{dt} = \left(J_{ion} + J_{rel} - J_{up}\right)/V_i, \quad \frac{dc_{up}}{dt} = \left(J_{up} - J_{tr}\right)/V_{up}, \quad \frac{dc_{rel}}{dt} = \left(J_{tr} - J_{rel}\right)/V_{rel},$$

where c, c_{up} and c_{rel} denote the Ca^{2+} concentration in the cytosol, the uptake pool and the release pool of the SR, respectively, with corresponding volumes V_i, V_{up} and V_{rel}. The three concentrations change due to the ionic flux J_{ion} across the plasma membrane, the release flux J_{rel} from the release pool into the cytosol, the uptake flux J_{up} from the cytosol into the uptake pool and the transfer flux J_{tr} from the uptake compartment to the release compartment.

The challenge for modelers lies in finding descriptions for all these fluxes, which often reflect mechanistic insights into the underlying dynamics. In this respect, compartmentalized models demand the same input as ODE models for averaged Ca^{2+} concentrations. One major difference, however, is that some of the fluxes that are assumed to be present across the entire cell in models for the averaged Ca^{2+} concentration only occur for certain compartments. For example, the uptake current is usually assumed to operate throughout a well-stirred cell, but is restricted to the uptake compartment in (DiFrancesco and Noble 1985). From a mechanistic point of view, the uptake current is often carried by sarco-endoplasmic Ca^{2+} ATPase (SERCA) pumps and can be described by

$$J_{up} = v_m \frac{c^2}{K^2 + c^2},$$

where v_m and K represent the maximal uptake current and the value of the Ca^{2+} concentration at which pumps work at half their maximal uptake rate (EC50), respectively. The above equation assumes that the Ca^{2+} flux is unidirectional and only determined by the cytosolic Ca^{2+} concentration. However, experimental measurements strongly suggest that firstly luminal Ca^{2+} feeds back to SERCA pump dynamics and secondly Ca^{2+} movement between the cytosol and the ER/SR proceeds along multiple distinct states of the SERCA pump molecule. These experimental results have led to more comprehensive models of SERCA pumps such as in (Sneyd et al. 2003; Shannon et al. 2004; Higgins et al. 2006; Koivumäki et al. 2009; Tran et al. 2009)

The advantage of compartmentalized models lies in the computational ease in accounting for largely varying Ca^{2+} concentrations and spatial gradients. A single point model cannot incorporate the different peak values and time courses of e.g. the subsarcolemmal and bulk Ca^{2+} concentration in cardiac myocytes. On the other hand, a two-compartment model accomplishes this easily.

Compartmentalized models have significantly advanced our understanding of Ca^{2+} handling and the interaction between the membrane potential and the intracellular Ca^{2+} concentration in cardiac myocytes (Shiferaw et al. 2003; Shannon et al. 2004; Shiferaw and Karma 2006; Koivumäki et al. 2011). However, deriving multi-compartment descriptions for intracellular Ca^{2+}

signaling suffers from two major shortcomings. Firstly, it is not clear a priori how many compartments are needed to account for experimental measurements. Different models use different numbers of compartments and yet describe the same physiology (see e.g. table 1 in (Fink et al. 2011)). Secondly, compartmentalized models depend on the volumes of the compartments. It might appear straightforward to estimate the volume of the dyadic cleft, but it is less intuitive where to draw the line between the junctional and non-junctional SR or the bulk and the subsarcolemmal cytosolic space. The last point illustrates the fact that some of the compartments do not correspond to actual physical entities but to functional units that organize Ca^{2+} handling. Moreover, the spatial extent of these functional compartments may change over time due to molecular interactions, which in turn renders the volume estimation difficult to make. A prime example for this scenario is the impact of buffers on Ca^{2+} release through IP_3 channels. Especially mobile buffers can increase the effective size of a microdomain around an open IP_3R cluster. Ca^{2+} buffers are molecules that bind Ca^{2+} and hence increase the cellular Ca^{2+} capacity. It is worth noting that more than 90% of cellular Ca^{2+} is buffered under normal conditions and that buffers significantly affect local and global Ca^{2+} signals (Keener and Sneyd 2001; Falcke 2003a; Dargan and Parker 2003; Zeller et al. 2009). In addition, varying the number of IP_3Rs in a cluster changes the functional volume and hence the dynamics of compartmentalized IP_3R clusters such as modeled in (Williams et al. 2008).

The conceptual simplicity of compartmentalized models makes them ideal candidates to start exploring cellular heterogeneity with low computational demand. However, no matter how many compartments are used and how sophisticated they are, any compartmentalized model suffers from the above shortcomings. The only way to circumvent these issues is to treat the cellular space as what it is: a continuous representation of a cell where the only boundaries are those of the plasma membrane and intracellular organelles. In the next section, we will examine some more realistic models of intracellular Ca^{2+} dynamics. However, a better representation of the physiological reality comes at a price. Larger computational overheads are required and more involved mathematical analysis is needed, if it is feasible at all.

Spatially extended cell models

Ca^{2+} waves, whether spontaneous or triggered, abortive or cell-wide, correspond to one of the most common forms of Ca^{2+} signals. To fully map the large dynamic repertoire of Ca^{2+} waves, modelers have to go beyond the framework of ODEs discussed so far and turn to partial differential equations (PDEs). In contrast to the ODEs discussed above where the Ca^{2+} concentration only depends on time, PDEs treat the Ca^{2+} concentration as dependent on both space x and time t, i.e. $c = c(x,t)$. In its simplest form, the spatio-temporal evolution of the Ca^{2+} concentration is captured by

$$\frac{\partial c}{\partial t} = D\frac{\partial^2 c}{\partial x^2} + f(c), \qquad (2)$$

where D denotes the (effective) diffusion coefficient of Ca^{2+} in the cytosol and f describes the local Ca^{2+} dynamics, i.e. Ca^{2+} release through IP_3Rs and RyRs or Ca^{2+} resequestration by SERCA pumps from the cytosol to the ER or SR. In this

respect, Ca^{2+} dynamics, as modeled by PDEs, has a direct connection to the ODEs outlined above, since the function f in equation (2) is the same as the right hand side of equation (1). The effective diffusion coefficient reflects the impact of Ca^{2+} buffers on Ca^{2+} transport. Essentially, Ca^{2+} diffuses through the cytosol either as a free ion or bound to mobile buffers. Since buffers are much larger than Ca^{2+}, buffer-bound Ca^{2+} diffuses more slowly than free Ca^{2+}. An effective diffusion coefficient accounts for these different transport velocities. One method to compute D is the fast buffer approximation (Wagner and Keizer 1994). To date, Ca^{2+} waves have been studied in great detail, and I refer the reader to (Sneyd and Tsaneva-Atanasova 2002; Falcke 2004) for recent reviews on Ca^{2+} wave propagation. Here, I would like to focus on some selected aspects of Ca^{2+} waves.

The main driving force behind Ca^{2+} waves is CICR. Suppose Ca^{2+} is liberated at one Ca^{2+} release site while all neighboring Ca^{2+} release sites are quiescent. Calcium then diffuses from the active Ca^{2+} release site to the dormant sites, which increases the probability of these channels to open. Once these channels open, Ca^{2+} is liberated and in turn diffuses to adjacent Ca^{2+} release sites where a new round of Ca^{2+} liberation is triggered. In this way, a saltatory Ca^{2+} wave propagates through a cell. For IP_3Rs, the notion of CICR is often illustrated by the bell-shaped dependence of the stationary open probability of the IP_3R on the cytosolic Ca^{2+} concentration (Bezprozvanny et al. 1991; Foskett et al. 2007). A small rise of the cytosolic Ca^{2+} concentration above base level leads to a significant increase in the IP_3R open probability. However, steady-state data do not necessarily capture the true dynamics of an IP_3R, neither is a bell-shaped dependence of the open probability necessary to explain observed Ca^{2+} signals (Sneyd and Falcke 2005). As a consequence, it is more appropriate to conceptualize CICR as Ca^{2+} excitability (Keizer et al. 1995). Borrowing ideas from nonlinear dynamical systems, Ca^{2+} excitability refers to the fact that Ca^{2+} liberation is only initiated at a cluster of closed Ca^{2+} releasing channels if the cluster state is sufficiently perturbed. One such perturbation is the increase in the cytosolic Ca^{2+} concentration, others include a rise of the IP_3 concentration or phosphorylation of the receptor molecules. One class of models for Ca^{2+} wave propagation that builds on the notion of a critical value of the cytosolic Ca^{2+} concentration to trigger Ca^{2+} release are those of the fire-diffuse-fire (FDF) type (Pearson and Ponce-Dawson 1998; Keizer et al. 1998; Dawson et al. 1999). Also known as threshold models, Ca^{2+} liberation starts as soon as the cytosolic Ca^{2+} concentration reaches a critical value. Calcium release continues for a fixed duration, comparable to the lifetime of a Ca^{2+} puff or spark, then the release site closes and becomes refractory. The beauty of FDF models is that they are amenable to a rigorous mathematical analysis and computationally inexpensive. The first property makes them ideal candidates to study large portions of parameter space since expressions for key features of traveling waves such as the wave speed are available in closed form. Instead of running a large number of simulations all that is needed is to evaluate analytical expressions, which can be done in a fraction of the time that is required for the numerical simulations. For example, the impact of SERCA pumps on Ca^{2+} wave propagation has been studied in (Coombes 2001), and investigating the interplay between the cytosol and the SR provided explanations for two novel wave types: tango waves (Li 2003; Thul et al. 2008b) and sensitization waves (Keller et al. 2007; Thul et al. 2009a). While deterministic models such as the original FDF description are still instrumental

in advancing our understanding of intracellular Ca^{2+} waves, hybrid frameworks that incorporate the stochastic nature of Ca^{2+} release have gained considerable attention. In this respect, threshold models are ideally suited to capture the random opening of IP_3Rs and RyRs, and study stochastic Ca^{2+} waves. In these models, the constant threshold for Ca^{2+} liberation is replaced by a fluctuating value which can in principle be derived from experiments (Izu et al. 2001; Coombes and Timofeeva 2003).

The above examples for Ca^{2+} waves all represent a cell as a one-dimensional line. From an experimentalist's point of view, this might appear to be a crude approximation to the real cellular shape and morphology. The value of one-dimensional models is their ability to identify key mechanisms of Ca^{2+} wave propagation and to provide a thorough mathematical underpinning of the intracellular processes that drive Ca^{2+} waves. In turn, this establishes confidence in the chosen modeling framework to explore two- and three-dimensional models while avoiding spurious results.

Coupled with the stochastic description of Ca^{2+} release, two-dimensional models of the intracellular Ca^{2+} concentration have provided intriguing insights into the generation and propagation of Ca^{2+} waves (see Figure 1). For example, a stochastic FDF model exhibits spatially synchronized oscillations, i.e. every point in the cell oscillates with the same phase as its neighbors and the averaged Ca^{2+} concentration shows regular oscillations (Coombes and Timofeeva 2003). However, as soon as the random opening of the Ca^{2+} releasing channels is turned off, the oscillations disappear. Although the cell-wide signal looks deterministic and homogenous, an ODE framework as discussed above fails to provide the right mechanism. It is the interplay between the spatial arrangement of the Ca^{2+} release channels and the fluctuations of channel opening that are important, neither of which are captured by ODEs. Similarly, the results in (Falcke 2003b) suggest that Ca^{2+} waves are initiated by the random formation of a critical nucleus. Only if a sufficient number of IP_3R clusters open at the same time in close proximity will a Ca^{2+} wave be born. Two-dimensional simulations have been instrumental in providing first estimates for the number of IP_3Rs per cluster, which is still hard to determine experimentally due to the small cluster diameter (Swillens et al. 1999; Shuai and Jung 2003a; 2003b), but see (Smith and Parker 2009) for a recent experimental measurement.

The success of two-dimensional simulations and the availability of more powerful computing facilities have promoted the study of Ca^{2+} signals in a three-dimensional cellular environment (Izu et al. 2006; Means et al. 2006; Rüdiger et al. 2007; Li and Holden 2009; Skupin et al. 2010; Solovey et al. 2011; Thurley and Falcke 2011; Thul et al. 2012). Each of these studies focuses on a particular aspect of Ca^{2+} signaling such as a realistic distribution of Ca^{2+} release sites, ER geometry, or the interaction of a small number of IP_3Rs and IP_3R clusters with detailed gating schemes. Taken together, this research provides a kaleidoscopic view of the nature of intracellular Ca^{2+} signals and highlights two of the main characteristics of intracellular Ca^{2+} dynamics. Firstly, intracellular Ca^{2+} is an intrinsic stochastic medium. The random state transitions that occur at a cluster of IP_3Rs is due to the continuous binding and unbinding of Ca^{2+} and IP_3 to a small number of binding sites and is instrumental in generating Ca^{2+} puffs. The large

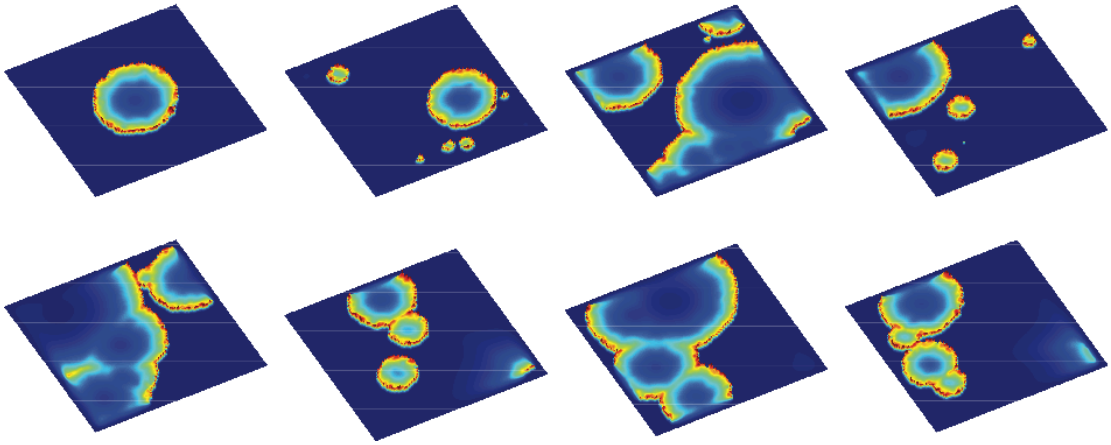

Figure 1: Ca^{2+} waves in a stochastic two-dimensional FDF model. The eight panels show snapshots of multiple Ca^{2+} waves (time runs from left to right, top to bottom). The first wave (top left) is triggered at the beginning of the simulation, while all other waves emerge spontaneously due to fluctuations of Ca^{2+} release. For a three-dimensional stochastic FDF model, I refer the reader to (Thul et al. 2012)

Ca^{2+} concentrations that occur at an open cluster saturate any deterministic binding dynamics and hence cannot explain experimentally observed puff statistics (Thul and Falcke 2004a; 2004b). As a consequence intracellular Ca^{2+} oscillations emerge at the cellular level through the stochastic orchestration of Ca^{2+} puffs. Single puff sites do not exhibit oscillatory dynamics (Thurley et al. 2011). Secondly, the true nature of Ca^{2+} dynamics can only be captured in spatially extended models. Microdomains and Ca^{2+} waves clearly indicate that cells are not well-stirred bioreactors where the Ca^{2+} concentration is the same across the entire cell. The generation and molecular read-out of Ca^{2+} signals depends on the local environment, not on properties of the bulk Ca^{2+} concentration.

The road ahead

Modeling intracellular Ca^{2+} dynamics has already come a long way and has significantly advanced our understanding of this most versatile second messenger. So far, we have gained great insight into individual levels of the Ca^{2+} signaling hierarchy, e.g. for Ca^{2+} blips, puffs and sparks or whole cell Ca^{2+} waves. The challenge for the future is to construct models that span the entire spatio-temporal range (Thurley et al. 2012). For IP_3 mediated Ca^{2+} patterns, this means computational frameworks that take us from the stochastic binding of Ca^{2+} and IP_3 to their respective binding sites on the IP_3R, to a cellular response accounting for the often irregular three-dimensional geometry of cells and the spatially heterogeneous expression of large numbers of IP_3R clusters. The constant advances in computational power will certainly help us to achieve this goal. At the same time, modelers have to improve existing models and to develop novel techniques that characterize intracellular Ca^{2+} dynamics more efficiently without sacrificing details of the Ca^{2+} signaling toolkit. Constructing models that are firmly rooted in experimental findings and successfully predict experimental results, while at the same time providing mechanistic interpretations of signaling pathways, will serve as a guiding principle for future research both in modeling and experiment.

References

Berridge MJ. 2006. Calcium microdomains: organization and function. *Cell Calcium* **40**: 405–412.

Berridge MJ, Lipp P, Bootman MD. 2000. The versatility and universality of calcium signalling. *Nat Rev Mol Cell Biol* **1**: 11–21.

Bers DM. 2002. Cardiac excitation-contraction coupling. *Nature* **415**: 198–205.

Bezprozvanny I, Watras J, Ehrlich BE. 1991. Bell-shaped calcium-response curves of Ins(1,4,5)P_3-gated and calcium-gated channels from endoplasmic-reticulum of cerebellum. *Nature* **351**: 751–754.

Bootman M, Niggli E, Berridge M, Lipp P. 1997. Imaging the hierarchical Ca^{2+} signalling system in HeLa cells. *J Physiol (Lond)* **499 (Pt 2)**: 307–314.

Cannell MB, Kong CHT. 2012. Local control in cardiac E-C coupling. *J Mol Cell Cardiol* **52**: 298–303.

Coombes S. 2001. The effect of ion pumps on the speed of travelling waves in the fire-diffuse-fire model of Ca^{2+} release. *Bull Math Biol* **63**: 1–20.

Coombes S, Timofeeva Y. 2003. Sparks and waves in a stochastic fire-diffuse-fire model of Ca^{2+} release. *Phys Rev E* **68**: 021915.

Dargan SL, Parker I. 2003. Buffer kinetics shape the spatiotemporal patterns of IP_3-evoked Ca^{2+} signals. *J Physiol (Lond)* **553**: 775–788.

Dawson SP, Keizer J, Pearson JE. 1999. Fire-diffuse-fire model of dynamics of intracellular calcium waves. *Proc Natl Acad Sci USA* **96**: 6060–6063.

De Young GW, Keizer J. 1992. A single-pool inositol 1,4,5-trisphosphate-receptor-based model for agonist-stimulated oscillations in Ca^{2+} concentration. *Proc Natl Acad Sci USA* **89**: 9895–9899.

DiFrancesco D, Noble D. 1985. A model of cardiac electrical activity incorporating ionic pumps and concentration changes. *Philos Trans R Soc Lond, B, Biol Sci* **307**: 353–398.

Dupont G, Abou-Lovergne A, Combettes L. 2008. Stochastic aspects of oscillatory Ca^{2+} dynamics in hepatocytes. *Biophys J* **95**: 2193–2202.

Dupont G, Combettes L, Bird GS, Putney JW. 2011. Calcium oscillations. *Cold Spring Harb Perspect Biol* **3**: pii: a004226.

Falcke M. 2003a. Buffers and oscillations in intracellular Ca^{2+} dynamics. *Biophys J* **84**: 28–41.

Falcke M. 2003b. On the role of stochastic channel behavior in intracellular Ca^{2+} dynamics. *Biophys J* **84**: 42–56.

Falcke M. 2004. Reading the patterns in living cells - the physics of Ca^{2+} signaling. *Adv Phys* **53**: 255–440.

Fink M, Niederer SA, Cherry EM, Fenton FH, Koivumäki JT, Seemann G, Thul R, Zhang H, Sachse FB, Beard D, et al. 2011. Cardiac cell modelling: observations from the heart of the cardiac physiome project. *Prog Biophys Mol Bio* **104**: 2–21.

Foskett JK, White C, Cheung K-H, Mak D-OD. 2007. Inositol trisphosphate receptor Ca^{2+} release channels. *Physiol Rev* **87**: 593–658.

Goldbeter A, Dupont G, Berridge MJ. 1990. Minimal model for signal-induced Ca^{2+} oscillations and for their frequency encoding through protein phosphorylation. *Proc Natl Acad Sci USA* **87**: 1461–1465.

Higgins ER, Cannell MB, Sneyd J. 2006. A buffering SERCA pump in models of calcium dynamics. *Biophys J* **91**: 151–163.

Izu LT, Means SA, Shadid JN, Chen-Izu Y, Balke CW. 2006. Interplay of ryanodine receptor distribution and calcium dynamics. *Biophys J* **91**: 95–112.

Izu LT, Wier WG, Balke CW. 2001. Evolution of cardiac calcium waves from stochastic calcium sparks. *Biophys J* **80**: 103–120.

Keener J, Sneyd J. 2001. *Mathematical Physiology*. Springer.

Keizer J, Li YX, Stojilković S, Rinzel J. 1995. $InsP_3$-induced Ca^{2+} excitability of the endoplasmic reticulum. *Mol Biol Cell* **6**: 945–951.

Keizer J, Smith G, Ponce Dawson S, Pearson J. 1998. Saltatory propagation of Ca^{2+} waves by Ca^{2+} sparks. *Biophys J* **75**: 595–600.

Keller M, Kao JPY, Egger M, Niggli E. 2007. Calcium waves driven by "sensitization" wave-fronts. *Cardiovasc Res* **74**: 39–45.

Koivumäki JT, Korhonen T, Tavi P. 2011. Impact of sarcoplasmic reticulum calcium release on calcium dynamics and action potential morphology in human atrial myocytes: a computational study. *PLoS Comput Biol* **7**: e1001067.

Koivumäki JT, Takalo J, Korhonen T, Tavi P, Weckström M. 2009. Modelling sarcoplasmic reticulum calcium ATPase and its regulation in cardiac myocytes. *Philos Transact A Math Phys Eng Sci* **367**: 2181–2202.

Li P, Holden AV. 2009. Intracellular Ca^{2+} nonlinear wave behaviours in a three dimensional ventricular cell model. *Physcia D* **238**: 992–999.

Li Y. 2003. Tango waves in a bidomain model of fertilization calcium waves. *Physcia D* **186**: 27–49.

Li Y, Rinzel J. 1994. Equations for $InsP_3$ receptor-mediated $[Ca^{2+}]_i$ oscillations

derived from a detailed kinetic model: a Hodgkin-Huxley like formalism. *J Theor Biol* **166**: 461–473.

Mak D-OD, McBride SMJ, Foskett JK. 2003. Spontaneous channel activity of the inositol 1,4,5-trisphosphate ($InsP_3$) receptor ($InsP_3R$). Application of allosteric modeling to calcium and $InsP_3$ regulation of $InsP_3R$ single-channel gating. *J Gen Physiol* **122**: 583–603.

Means S, Smith AJ, Shepherd J, Shadid J, Fowler J, Wojcikiewicz RJH, Mazel T, Smith GD, Wilson BS. 2006. Reaction diffusion modeling of calcium dynamics with realistic ER geometry. *Biophys J* **91**: 537–557.

Meyer T, Stryer L. 1988. Molecular-Model for Receptor-Stimulated Calcium Spiking. *Proc Natl Acad Sci USA* **85**: 5051–5055.

Parekh AB. 2011. Decoding cytosolic Ca^{2+} oscillations. *Trends Biochem Sci* **36**: 78–87.

Parker I, Yao Y. 1996. Ca^{2+} transients associated with openings of inositol trisphosphate-gated channels in Xenopus oocytes. *J Physiol (Lond)* **491 (Pt 3)**: 663–668.

Pearson JE, Ponce-Dawson S. 1998. Crisis on skid row. *Physica A* **257**: 141–148.

Rüdiger S, Shuai JW, Huisinga W, Nagaiah C, Warnecke G, Parker I, Falcke M. 2007. Hybrid stochastic and deterministic simulations of calcium blips. *Biophys J* **93**: 1847–1857.

Shannon TR, Wang F, Puglisi J, Weber C, Bers DM. 2004. A mathematical treatment of integrated Ca dynamics within the ventricular myocyte. *Biophys J* **87**: 3351–3371.

Shiferaw Y, Karma A. 2006. Turing instability mediated by voltage and calcium diffusion in paced cardiac cells. *Proc Natl Acad Sci USA* **103**: 5670–5675.

Shiferaw Y, Watanabe MA, Garfinkel A, Weiss JN, Karma A. 2003. Model of intracellular calcium cycling in ventricular myocytes. *Biophys J* **85**: 3666–3686.

Shuai J, Pearson JE, Foskett JK, Mak D-OD, Parker I. 2007. A Kinetic Model of Single and Clustered IP_3 Receptors in the Absence of Ca^{2+} Feedback. *Biophys J* **93**: 1151–1162.

Shuai J-W, Jung P. 2002. Stochastic properties of Ca^{2+} release of inositol 1,4,5-trisphosphate receptor clusters. *Biophys J* **83**: 87–97.

Shuai JW, Jung P. 2003a. Optimal ion channel clustering for intracellular calcium signaling. *Proc Natl Acad Sci USA* **100**: 506–510.

Shuai JW, Jung P. 2003b. Selection of intracellular calcium patterns in a model with clustered Ca^{2+} release channels. *Phys Rev E* **67**: 031905.

Skupin A, Falcke M. 2009. From puffs to global Ca^{2+} signals: how molecular properties shape global signals. *Chaos* **19**: 037111.

Skupin A, Kettenmann H, Falcke M. 2010. Calcium signals driven by single channel noise. *PLoS Comput Biol* **6**: e1000870.

Smith IF, Parker I. 2009. Imaging the quantal substructure of single IP_3R channel activity during Ca^{2+} puffs in intact mammalian cells. *Proc Natl Acad Sci USA* **106**: 6404–6409.

Sneyd J, Dufour J-F. 2002. A dynamic model of the type-2 inositol trisphosphate receptor. *Proc Natl Acad Sci USA* **99**: 2398–2403.

Sneyd J, Falcke M. 2005. Models of the inositol trisphosphate receptor. *Prog Biophys Mol Bio* **89**: 207–245.

Sneyd J, Tsaneva-Atanasova K. 2002. Modeling Calcium Waves. In *Understanding Calcium Dynamics* (eds. M. Falcke and D. Malchow), pp. 179–199, Springer.

Sneyd J, Tsaneva-Atanasova K, Bruce J, Straub S, Giovannucci D, Yule D. 2003. A model of calcium waves in pancreatic and parotid acinar cells. *Biophys J* **85**: 1392–1405.

Soeller C, Cannell MB. 2004. Analysing cardiac excitation-contraction coupling with mathematical models of local control. *Prog Biophys Mol Bio* **85**: 141–162.

Solovey G, Fraiman D, Dawson SP. 2011. Mean field strategies induce unrealistic non-linearities in calcium puffs. *Front Physiol* **2**: 46.

Solovey G, Fraiman D, Pando B, Ponce Dawson S. 2008. Simplified model of cytosolic Ca^{2+} dynamics in the presence of one or several clusters of Ca^{2+} -release channels. *Phys Rev E* **78**: 041915.

Stern MD. 1992. Theory of excitation-contraction coupling in cardiac muscle. *Biophys J* **63**: 497–517.

Sun XP, Callamaras N, Marchant JS, Parker I. 1998. A continuum of $InsP_3$-mediated elementary Ca^{2+} signalling events in Xenopus oocytes. *J Physiol (Lond)* **509 (Pt 1)**: 67–80.

Swaminathan D, Ullah G, Jung P. 2009. A simple sequential-binding model for calcium puffs. *Chaos* **19**: 037109.

Swillens S, Dupont G, Combettes L, Champeil P. 1999. From calcium blips to calcium puffs: theoretical analysis of the requirements for interchannel communication. *Proc Natl Acad Sci USA* **96**: 13750–13755.

Taufiq-Ur-Rahman, Skupin A, Falcke M, Taylor CW. 2009. Clustering of $InsP_3$ receptors by $InsP_3$ retunes their regulation by $InsP_3$ and Ca^{2+}. *Nature* **458**: 655–659.

Thul R, Bellamy TC, Roderick HL, Bootman MD, Coombes S. 2008a. Calcium oscillations. *Adv Exp Med Bio* **641**: 1–27.

Thul R, Coombes S, Roderick HL, Bootman MD. 2012. Subcellular calcium dynamics in a whole-cell model of an atrial myocyte. *Proc Natl Acad Sci USA* **109**: 2150–2155.

Thul R, Coombes S, Smith GD. 2009a. Sensitisation waves in a bidomain fire-diffuse-fire model of intracellular Ca^{2+} dynamics. *Physcia D* **238**: 2142–2152.

Thul R, Falcke M. 2004a. Release currents of IP_3 receptor channel clusters and concentration profiles. *Biophys J* **86**: 2660–2673.

Thul R, Falcke M. 2004b. Stability of membrane bound reactions. *Phys Rev Lett* **93**: 188103.

Thul R, Smith GD, Coombes S. 2008b. A bidomain threshold model of propagating calcium waves. *J Math Biol* **56**: 435–463.

Thul R, Thurley K, Falcke M. 2009b. Toward a predictive model of Ca^{2+} puffs. *Chaos* **19**: 037108.

Thurley K, Falcke M. 2011. Derivation of Ca^{2+} signals from puff properties reveals that pathway function is robust against cell variability but sensitive for control. *Proc Natl Acad Sci USA* **108**: 427–432.

Thurley K, Skupin A, Thul R, Falcke M. 2012. Fundamental properties of Ca^{2+} signals. *Biochim Biophys Acta* **1820**: 1185–1194.

Thurley K, Smith IF, Tovey SC, Taylor CW, Parker I, Falcke M. 2011. Timescales of IP_3-evoked Ca^{2+} spikes emerge from Ca^{2+} puffs only at the cellular level. *Biophys J* **101**: 2638–2644.

Tran K, Smith NP, Loiselle DS, Crampin EJ. 2009. A thermodynamic model of the cardiac sarcoplasmic/endoplasmic Ca^{2+} (SERCA) pump. *Biophys J* **96**: 2029–2042.

Wagner J, Keizer J. 1994. Effects of Rapid Buffers on Ca^{2+} Diffusion and Ca^{2+} Oscillations. *Biophys J* **67**: 447–456.

Williams GSB, Molinelli EJ, Smith GD. 2008. Modeling local and global intracellular calcium responses mediated by diffusely distributed inositol 1,4,5-trisphosphate receptors. *J Theor Biol* **253**: 170–188.

Zalk R, Lehnart SE, Marks AR. 2007. Modulation of the ryanodine receptor and intracellular calcium. *Annu Rev Biochem* **76**: 367–385.

Zeller S, Rüdiger S, Engel H, Sneyd J, Warnecke G, Parker I, Falcke M. 2009. Modeling of the modulation by buffers of Ca^{2+} release through clusters of IP_3 receptors. *Biophys J* **97**: 992–1002.